IGARSS 2023 - 2023 IEEE International Geoscience and Remote Sensing Symposium | 979-8-3503-2010-7/23/$31.00 ©2023 IEEE | DOI: 10.1109/IGARSS52108.2023.10281803

# EXTREME WINDS FROM KU-BAND AND C-BAND WIND SCATTEROMETERS

*Xingou Xu[1], Ad Stoffelen[2]*, Weicheng Ni[3], Marcos Portabella[4] and Alberto Rabaneda[5]*

1. Key Laboratory of Microwave Remote Sensing, National Space Science Center, CAS, Beijing, 100190, China
2. Royal Netherlands Meteorological Institute （KNMI）, 3730 AE, De Bilt, Utrecht, The Netherlands
3. National University of Defense Technology, Changsha 410073, China
4. Barcelona Expert Centre (BEC), Institut de Ciències del Mar (ICM-CSIC) Barcelona, Spain
5. Norwegian Meteorological Institute (MET Norway), Oslo, Norway

* ad.stoffelen@knmi.nl

## ABSTRACT

C-band scatterometer winds have been adjusted for extreme conditions and in this research extension to Ku-band scatterometers is investigated. With rain rates from the Global Precipitation Measurement mission collocated to the Ku-band scatterometer observations to identify and exclude rain contamination of winds, calibration of the Ku-band observations can be done. Using high-wind cases extracted from collocated C- and Ku-band observations, we develop a calibration model and extend the Ku-band winds to 35 m/s. Validation is obtained from the set not included in the model derivation, indicating a speed error less than 10% for wind speed larger than 30m/s. The modified speed is consistent with the Step Frequency Microwave Radiometer measurements, when collocated with another Ku-band scatterometer. A comparison for the Tropical Cyclone Man-yi in 2018 shows the adjustedd wind fits better with the best-track information provided by the Chinese Meteorological Administration, while more details are revealed. Results can be improved after obtaining more collocations with the dual-frequency scatterometer "*WindRad*" onboard the FY-3E satellite. A method for wind direction enhancement in extreme conditions is also discussed.

***Index Terms—*** wind scatterometers, Ku-band and C-band collocations, extreme wind speed adjustment

## 1. INTRODUCTION

Tropical cyclones (TC) or hurricanes cause severe damage during their landfalls. In China, the average 9.3 landfall TCs cause more than ＄10 billion property loss, while taking thousands of human lives each year [1]. At the same time, remotely-sensed data with large coverage have the potential of providing vital information for improved forecasts. Among them, scatterometers have been providing high-quality ocean surface wind products for more than 40 years [2], while exploring extreme-wind retrieval quality is ongoing. Recently, with reference to the Step-Frequency-Microwave Radiometer (SFMR) products, the good quality of the C-band extreme wind speeds has been well proven [3] and extension to Ku-band scatterometers is ongoing, tackling the problem of contamination by precipitation. In this research, we confirm that rain contamination causes the retrieved winds to deviate from other wind observations, when stratified against the co-registered rain rates from the Global Precipitation Measurement (GPM). A calibration method has been developed and the resulting Ku-band winds validated with reference to the C-band collocations. The high wind collocations are extracted with information from the International Best Track Archive for Climate Stewardship (IBTrACS), and rain is excluded by using the KNMI product quality control (QC). The validation by the validation set (i.e., the set not applied in the model development) shows errors lower than 10% for wind speeds larger than 30m/s. An example for tropical cyclone Man-yi is highlighted from the validation set and compared with the maximum wind speed from the best-track information provided by the Chinese Meteorological Administration (CMA), indicating better consistency than existing (unadjusted) products. Furthermore, improved extreme wind vector retrieval is being explored by resolution enhancement with reference to Synthetic Aperture Radar (SAR) images that capture more dynamic spatial details [4]. Beyond the current research exploiting C-band collocations, the improvements in wind vector quality for Ku-band extreme winds will be explored, as discussed in this manuscript.

## 2. METHOD

First, both C-band scatterometer data sets are calibrated against SFMR using a well-explored methodology, in the equation for wind speed larger than 12 m/s [3]:

$$U^*_{10s} = 0.0095U^2_{10s} + 1.52U_{10s} - 7.6 \qquad (1)$$

Where $U_{10s}$ is the stress-equivalent wind retrieved with the CMOD7 GMF, and $U^*_{10s}$ is the stress-equivalent wind adjusted for high wind conditions. Subsequently, the Ku-band observations are collocated with C-band for high wind conditions, as extracted from the best track information. With co-registered rain rates, the collocations are compared to obtain the Ku-band performances in extreme conditions, where a calibration model is derived following the results. Collocations without GPM are used for validation.

The Ku-band scatterometer observations are obtained from the OSCAT-2 scatterometer onboard SCATSAT-1, while the C-band collocations are from ASCAT-A and ASCAT-B onboard Metop-A and Metop-B satellites, respectively. The data covers the range from October 2016 to January 2019 [5], [6]. Then the high wind cases are extracted with reference to the best track data from IBTrACS globally [7]. Simultaneous rain rates are from the GPM post processed high-quality products [8]. In all, 1,167,846 and 746,855 WVCs of OSCAT-2 collocations with, respectively, ASCAT-A and ASCAT-B are obtained under TC conditions, including 43,472 and 37,623 WVCs, respectively, with rain collocations. When the traditional strict QC employing the MLE indicator [9] is adopted, and the rain screening from $J_{oss}$ [10] is not applied, respectively, 38,242 and 33,261 are accepted by both the Ku- and C-band QC (QC-I) with collocated rain rate. Finally, there are 34,606 and 30,407 WVCs, respectively, with 0 mm/h rain rate, and these are used for the Ku-band calibration model. The time lag for scatterometers is half an hour, and for GPM rain co-registration it is 4.8 minutes at maximum.

Further validation is conducted with the SFMR data collocated with the Ku-band scatterometer HSCAT onboard the HY-2B satellite in the year 2019 [11], [12]. Direct matches have been sought, limiting the distance to the centre of the WVC to be within 17.6 km and 30 minutes in time. In total, 363 WVCs are obtained while 150 WVCs are accepted by the HSCAT QC, with a corresponding maximum wind speed of SFMR of 32.89 m/s.

### 3. EXPERIMENTS AND RESULTS

Fig.1 is plotted from the data set with rain collocations for all QC conditions. The horizontal axis is the Ku-band wind speed and the vertical axis is the collocated C-band with dropsonde-adjusted wind speeds [3]. The color shows the rain information from GPM. It can be observed that higher rain rates constitute the bulging part of Ku- and C-band collocations from about 15 m/s to about 20 m/s in the Ku-band speed. Fig.2 further verifies this, where the horizontal and vertical axes are rain rate and the calibrated C-band wind speed, and the color represents the differences between the Ku-band GMF model and the observed normalized radar cross-section (NRCS) from the firstly stored NRCS in Level 2 product in horizontal polarized in receiving and transmitting (*HH*) in dB. Note that the color palette is limited to the range of -10 and 5 dB, where most differences are fit in. In correspondence with Fig.1, the deviations are well populated around the wind speed at Ku-band with the higher rain rates in Fig. 2, and the colors are mostly blueish for lower wind speed and red for higher speed in general below 35 m/s for the adjusted C-band winds, indicating resp. an underestimation and overestimation of wind speed, an obvious example is that rain causes the wind retrieval procedure overestimate the winds from about 11 m/s to below about 23 m/s, which is consistent with the curvature in Fig.1.

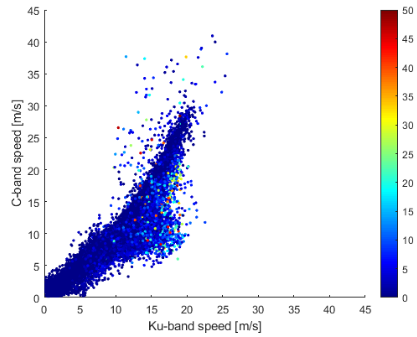


Fig.1 Scatterplot of collocated C-band (adjusted) versus Ku-band winds, where the color represents the collocated GPM rain rate.

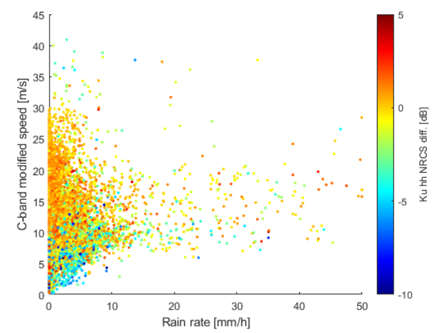


Fig. 2. The joint probability density function of collocated C-band (adjusted) wind and GPM rain, where the color represents the NRCS differences.

Considering the sample distribution, for wind speeds below 35 m/s, and using the QC-I data set of rain co-registration, but only for GPM rain rates of 0 mm/h, the calibration function of the Ku-band is derived using collocated C-band adjusted winds, as follows:

$$U_{10s}^{*} = -2.421 * 10^{-5} * U_{10s}^{5} + 0.001122 * U_{10s}^{4} - 0.015 * U_{10s}^{3} + 0.07096 * U_{10s}^{2} + 0.8604 * U_{10s} + 0.1767; \quad (2)$$

Fig. 3 shows the scatterplots of the intercalibrated Ku- and C-band winds, for the intercalibration set (a) and the independent validation set (b). . Although the intercalibration set lacks data between 30 and 35 m/s (a), the fit proves effective at such wind range as shown in the validation set (b). Note also that the latter doesn't contain GPM rain collocations, and it only considers the Ku-band QC flag to discard potentially rain contaminated WVCs.

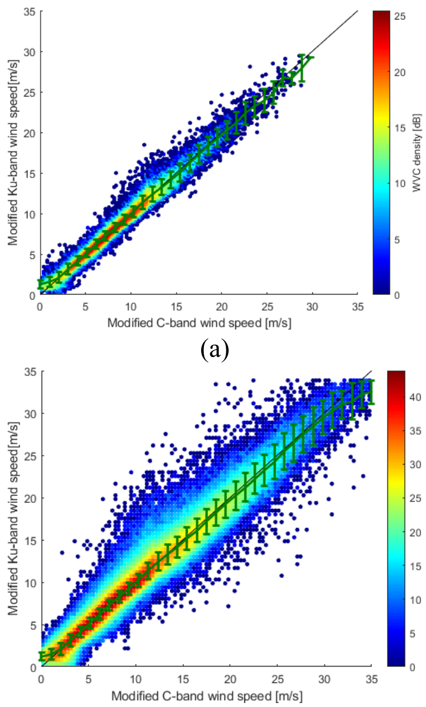


(a)

(b)

Fig.3 Scatterplots of adjusted Ku-band (using eq. 2) versus adjusted C-band (using eq. 1) winds, for the intercalibration set (a) and the validation set(b),. The color indicates WVC densities in dB.

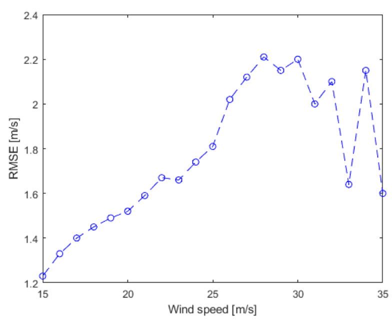


Fig.4 OSCAT2 - ASCAT RMSD of the intercalibrated Ku-band and C-band wind speeds for the validation set as a function of binned ASCAT adjusted speed.

Fig. 4 shows the binned Root Mean Squared Difference (RMSD) of the fit against the C-band collocations, for wind speeds larger than 15 m/s. It can be seen that the RMSD is the largest between 22 m/s and 32 m/s, i.e., about 2.2 m/s. The fluctuating values above 32 m/s may be due to lack of samples. When applying Eq. (2) to the HSCAT speeds and collocating them with SFMR winds from 2019, the 150 WVCs passing QC are plotted in Fig. 5:

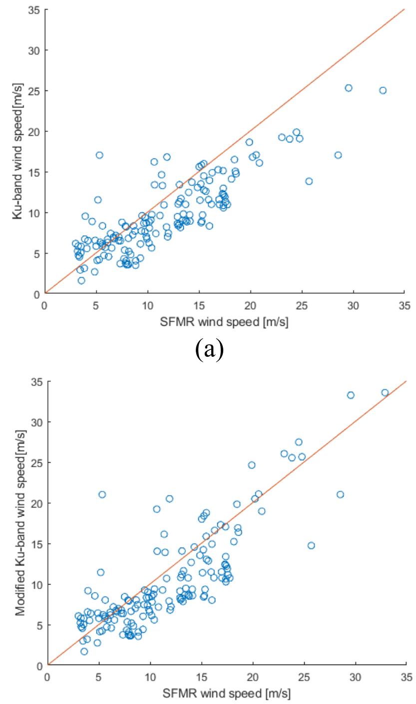


(a)

(b)

Fig.5 Scatter plot of the collocated nominal (a) and adjusted (b) Ku-band wind speed against collocated SFMR wind speed.

From Fig.5, it can be observed that the intercalibrated Ku-band winds better fit the SFMR observations than the nominal Ku-band winds, in the more reliable SFMR wind range above 20 m/s, while for the lower wind part, an HSCAT wind underestimation can be observed, both for the nominal and adjusted wind products.

Finally, the case of TC Man-yi is provided in Fig. 6, where the left panel corresponds to the nominal Ku-band wind speed and the right panel corresponds to the adjusted wind. The color represents wind speeds in m/s. In the observed scene, the closest maximum wind speed provided by the best-track information from the Chinese Meteorological Center (CMA) is 30 m/s, which is more consistent with the adjusted winds. In addition, especially in the red box region, the amplified winds by Eq. 2 (right panel) reveal enhanced details of this TC.

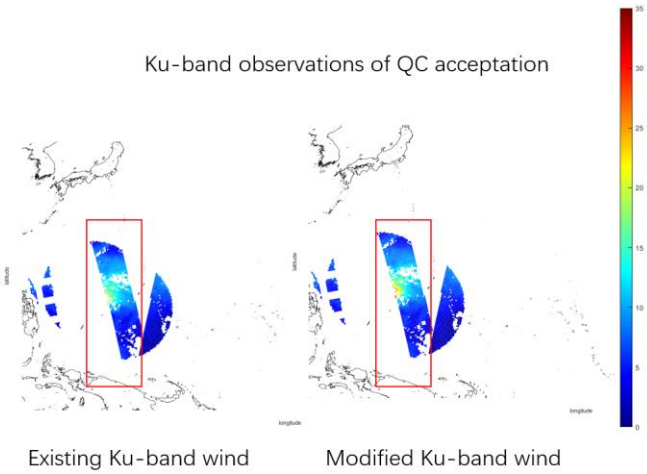


Fig. 6 HSCAT (on HY-2B) Ku-band nominal (left) and adjusted (right) winds for an overpass of TC Man-yi in 2018.

## 4. DISCUSSIONS

In this research, an intercalibration method for the Ku-band scatterometer wind speed has been developed and validated up to 35 m/s using ASCAT adjusted winds. The main effect casting doubt on the quality of Ku-band derived winds in extreme conditions is the presence of rain, as confirmed in this manuscript. For speeds higher than 35 m/s, limited sampling appears. These extreme winds tend to appear in a narrow eye wall region, necessitating rather precise collocation and co-registration procedures. Further research would be focusing on this and extend the calibration to larger winds.

Furthermore, after wind speed intercalibration, wind direction retrieval in TCs can be improved with reference to SAR data for resolution enhancement [13]. In addition, for Ku-band scatterometers the QC indicator $J_{oss}$ can be exploited and applied for an improved rain identification.

## 5. ACKNOWLEDGEMENT

This research is partly supported by the Feng-Yun Application Pioneering Project from China Meteorological Administration (Grant FY-APP-2022.0109).

## 6. REFERENCES

[1] L. Zhou, D. Chen, X. Lei. Progress and perspective on interactions between ocean and typhoon (in Chinese). Chin Sci Bull, 2019, 64:60–72, doi: 10.1360/N972018-00668

[2] A. Stoffelen, R. Kumar, J. Zou, V. Karaev, P. S. Chang and E. Rodriguez. Ocean Surface Vector Wind Observations, Springer International Publishing: 429-447, 2019. DOI 10.1007/978-3-319-94067-0_24

[3] F. Polverari, M. Portabella, W. Lin, J. W. Sapp, A. Stoffelen, Z. Jelenak, and P. S. Chang, “On High and Extreme Wind Calibration Using ASCAT,” IEEE Transactions on Geoscience and Remote Sensing, vol. 60, pp. 1-10, 2022.

[4] W. Ni, A. Stoffelen and K. Ren, "Tropical Cyclone Wind Direction Retrieval From Dual-Polarized SAR Imagery Using Histogram of Oriented Gradients and Hann Window Function," in IEEE Journal of Selected Topics in Applied Earth Observations and Remote Sensing,vol. 16, pp. 878-888, 2023, doi: 10.1109/JSTARS.2022.3230441.

[5] E. Directory. “SCATSat-1—Satellite Missions”. Accessed: Jan. 13rd, 2023. [Online]. Available: https://directory.eoportal.org/web/eoportal/satellite-missions/s/scatsat-1

[6] Eumetsat. (2018). ASCAT—EUMETSAT. Accessed: Jan. 13rd, 2023. [Online]. Available: https://www.eumetsat.int/ascat

[7] R. K. Knapp, H. J. Diamond, Howard J., J. P. Kossin, C. M. Kruk, C. J. Schreck, International Best Track Archive for Climate Stewardship (IBTrACS) Project, Version 4. [global]. NOAA National Centers for Environmental Information. https://doi.org/10.25921/82ty-9e16 [Jan. 2023].

[8] G. J. Huffman, D. T. Bolvin, and E. J. Nelkin, “Integrated Multi-satellitE Retrievals for GPM (IMERG) technical documentation,” NASA/GSFC Code, vol. 612, p. 47, Jun. 2015

[9] M. Portabella and A. Stoffelen, “Characterization of residual information for SeaWinds quality control,” IEEE Trans. Geosci. Remote Sens., vol. 40, no. 12, pp. 2747–2759, Dec. 2002, doi: 10.1109/ tgrs.2002.807750.

[10] X. Xu, and A. Stoffelen, “Improved Rain Screening for Ku-Band Wind Scatterometry,” IEEE Transactions on Geoscience and Remote Sensing, vol. 58, no. 4, pp. 2494-2503, 2020.

[11] J. Sapp, S. Alsweiss, Z. Jelenak, P. Chang, and J. Carswell, “Stepped Frequency Microwave Radiometer Wind-Speed Retrieval Improvements,” Remote Sensing, vol. 11, no. 3, p. 214, Jan. 2019.

[12] HY-2B: online accessed May, 2023 https://space.oscar.wmo.int/satellites/view/hy_2b

[13] Ni, W.; Stoffelen, A.; Ren, K.; Yang, X.; Vogelzang, J. SAR and ASCAT Tropical Cyclone Wind Speed Reconciliation. Remote Sens. 2022, 14, 5535.https://doi.org/10.3390/rs14215535